



HAL
open science

First experimental realization of the Dirac oscillator

John-Alexander Franco-Villafaña, Emerson Sadurni, Sonja Barkhofen, Ulrich Kuhl, Fabrice Mortessagne, Thomas H. Seligman

► **To cite this version:**

John-Alexander Franco-Villafaña, Emerson Sadurni, Sonja Barkhofen, Ulrich Kuhl, Fabrice Mortessagne, et al.. First experimental realization of the Dirac oscillator. *Physical Review Letters*, 2013, 111, pp.170405. 10.1103/PhysRevLett.111.170405 . hal-00840274v1

HAL Id: hal-00840274

<https://hal.science/hal-00840274v1>

Submitted on 2 Jul 2013 (v1), last revised 4 Nov 2013 (v2)

HAL is a multi-disciplinary open access archive for the deposit and dissemination of scientific research documents, whether they are published or not. The documents may come from teaching and research institutions in France or abroad, or from public or private research centers.

L'archive ouverte pluridisciplinaire **HAL**, est destinée au dépôt et à la diffusion de documents scientifiques de niveau recherche, publiés ou non, émanant des établissements d'enseignement et de recherche français ou étrangers, des laboratoires publics ou privés.

First experimental realization of the Dirac-Moshinsky oscillator

J. A. Franco-Villafaña,¹ E. Sadurní,² S. Barkhofen,³ U. Kuhl,⁴ F. Mortessagne,⁴ and T. H. Seligman^{1,5}

¹*Instituto de Ciencias Físicas, Universidad Nacional Autónoma de México,
Av. Universidad s/n, 62210 Cuernavaca, México*

²*Instituto de Física, Benemérita Universidad Autónoma de Puebla, Apartado Postal J-48, 72570 Puebla, México*

³*Fachbereich Physik, Philipps-Universität Marburg, Renthof 5, 35032 Marburg, Germany*

⁴*Laboratoire de Physique de la Matière Condensée, Université de Nice-Sophia Antipolis,
CNRS, UMR 7336 Parc Valrose - 06108 Nice, France*

⁵*Centro Internacional de Ciencias, 62210 Cuernavaca, México*

We present the first experimental microwave realization of the one-dimensional Dirac-Moshinsky oscillator, a paradigm in exactly solvable relativistic systems. The experiment relies on a relation of the Dirac-Moshinsky oscillator to a corresponding tight-binding system. This tight-binding system is implemented as a microwave system by a chain of coupled dielectric disks, where the coupling is evanescent and can be adjusted appropriately. The resonances of the finite microwave system yields the spectrum of the one-dimensional Dirac-Moshinsky oscillator with and without mass term. The flexibility of the experimental set-up allows the implementation of other one-dimensional Dirac type equations.

PACS numbers: 03.65.Pm, 07.57.Pt, 41.20.-q, 73.22.Pr

The relativistic version of the harmonic oscillator has been touched upon occasionally [1, 2], but became a widely used model for relativistic equations with the appearance of the seminal paper [3]. Originally it was known as the Dirac oscillator and later as the Dirac-Moshinsky oscillator (DMO) [4, 5]. Indeed since then the number of papers using this model has increased rapidly, mainly in mathematical physics [6–19], but also in nuclear physics [20–22], subnuclear physics [23, 24] and quantum optics [25–28]. In mathematical physics it has become the paradigm for the construction of covariant quantum models with some well determined non-relativistic limit, but has also attracted much attention in the environment of exactly solvable models and symmetries; it is amusing to mention that even the Higgs symmetry has been considered in this context [29].

While this model is a paradigm of mathematical physics, it does not describe a known physical system, as is the case for the Dirac equation for the hydrogen atom. Thus an experimental realization by other means is highly desirable. There are two proposals to realize analogue experiments. One in the realm of quantum optics [26–28] and the other one using a classical microwave setup [30]. In this paper we shall present a microwave realization for the 1-D DMO. Beyond its intrinsic interest, the experiment is also a starting point for further experimental exploration of Dirac like equations.

We will mainly follow the proposition of Ref. [30] but use a slightly different mechanism to appropriately take into account the finiteness of the experimental system. The experimental idea is based on a mapping of the DMO to a tight-binding model with dimers. In this model it is important that only nearest neighbor interactions are present. It consists of a chain of coupled disks with a high index of refraction sandwiched between two metal

lic plates. The coupling constants between the disks have to be adjusted properly, to obtain a spectrum which is equivalent to the DMO spectrum. This set-up has been used to investigate the Dirac points [31], disorder effects [32] and topological transitions in graphene [33]. We start with a short introduction to the DMO and its relation to a tight-binding hamiltonian with nearest neighbor coupling only. Thereafter we introduce the experimental setup and present the experimental results.

Dirac-Moshinsky oscillator.— The system that we now call the DMO was proposed more than 20 years ago [3, 34–37], and its properties and possible applications have been studied extensively. The original formulation was presented in hamiltonian form. Covariance was easily achieved and the physicality of such a system could be attained by means of a Pauli coupling [3]. In the present paper we will use the 1 + 1 dimensional version of the Dirac oscillator [4], which can be treated analogously and yields a two component spinless structure.

The system in question can be conceived in its simplest form by writing the corresponding hamiltonian as a function of the spectrum generating algebra. Let a, a^\dagger be the ladder operators of a non-relativistic harmonic oscillator and $\sigma_\pm = \sigma_x \pm i\sigma_y$ the creation and annihilation operators of spin 1/2 in terms of Pauli matrices. The 1 + 1 dimensional DMO hamiltonian is

$$H = \sigma_+ a + \sigma_- a^\dagger + \mu \sigma_z, \quad (1)$$

where the spectrum is given by

$$\epsilon_{\pm, n} = \pm \sqrt{n + \mu^2} \quad (2)$$

where the sign denotes particles and antiparticles. The dimensionless commutator $[a, a^\dagger] = 1$ ensures, that for a particle of mass m and an oscillator of frequency ω , we have $\mu = \sqrt{mc^2/\hbar\omega}$. Thus in the appropriate units,

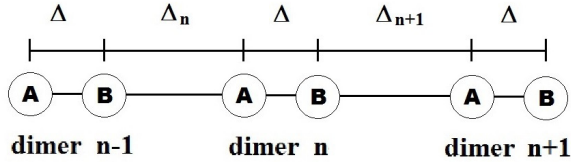


FIG. 1. A chain of resonators in dimeric configuration, with atoms of type A and B. The index n stands for the dimer number, Δ is the coupling between elements of the same dimer (intra-dimer coupling, kept constant throughout the array) and Δ_n is the coupling between the right end of dimer n and the left end of dimer $n+1$ (inter-dimer coupling). Have in mind that here we present the couplings only, later on $\Delta \leq \Delta_n$, which means that in the experiment the intra-dimer distance is the largest distance in the chain.

μ gives the mass of the particle directly, and the time variable scales as $t \mapsto \sqrt{\omega mc^2/\hbar}t$. In a certain limit, the DMO can also be reduced to the Weyl equation with a linear potential, thus one may call this system even a Weyl oscillator. Taking $m \rightarrow 0$ leaving $m\omega = \text{constant} \neq 0$ leads to $\mu \rightarrow 0$ and the following massless hamiltonian

$$H = \sigma_+ a + \sigma_- a^\dagger, \quad (3)$$

with the simplified spectrum

$$\epsilon_n = \pm\sqrt{n}. \quad (4)$$

Note here that for $n = 0$ there is a double degeneracy, where one of the states is given by $|-, 0\rangle$. Both hamiltonians (2) and (3) can be described within a tight-binding model with dimers.

Description as a tight-binding model.- The eigenvalue problem resulting from the hamiltonian (1) can be written as two coupled tight-binding equations of the form

$$\sqrt{n+1}\psi_{n+1}^- + \sqrt{n}\psi_{n-1}^+ + \mu\psi_n^+ = \epsilon_n\psi_n^+ \quad (5)$$

$$\sqrt{n}\psi_{n-1}^+ + \sqrt{n+1}\psi_{n+1}^- - \mu\psi_n^- = \epsilon_n\psi_n^- \quad (6)$$

where Ψ_n^\pm is the atomic wavefunction of the n -th dimer and the superscripts $+$ and $-$ indicate sites of type A and B (see also fig. 1). In our previous work [30] we have established that this model can be emulated in a one-dimensional chain with nearest neighbor interactions where the spin (\pm superscripts in the equations above) can be represented by A and B sites in a linear chain. By defining the new operators

$$b = \Delta(1+a), \quad b^\dagger = \Delta(1+a^\dagger), \quad (7)$$

the hamiltonian for a tight-binding chain of two species can be written as

$$H_{\text{chain}} = \sigma_+ b + \sigma_- b^\dagger + \mu\sigma_z \quad (8)$$

and μ is now the energy difference between the resonances sitting upon A and B sites giving rise to a spectral gap.

The constant Δ is nothing else than the coupling between two sites, and the spectrum of the system can be extracted by virtue of the algebraic relation $[b, b^\dagger] = \Delta^2$. As before, we have

$$\epsilon_n = \pm\sqrt{\Delta^2 n + \mu^2} \quad (9)$$

The map between the DMO and the coupled linear chain of two species is therefore quite natural. Finally we can see that the resulting array comprises dimers AB , e.g. sites A is always equally coupled to site B by Δ independently on n , whereas the coupling between the dimers Δ_n has to follow a specific law derived below. The requirements for a realization of b, b^\dagger , on the other hand, introduce the following restrictions: For the inter-dimer coupling $\Delta_n = \Delta\sqrt{n}$.

An appropriate cut-off.- Till now we assumed a semi-infinite array which terminates at one end with the value $\Delta_0 = 0$ (no more dimers to the left). Therefore, couplings of the form \sqrt{n} range from 0 to $\lim_{n \rightarrow \infty} \Delta_n = \infty$. However, experimentally accessible couplings always have an upper limit Δ_{sup} determined by the physical situation and such a restriction introduces a natural cut-off in the array by means of the relation $\Delta_{\text{sup}} = \Delta\sqrt{n_{\text{sup}}}$. Thus we arrive at a finite chain with a total number $2n_{\text{sup}}$ of sites.

A previously proposed finite realization [30], although well conceived for the infinite case, did not take into account cut-off effects appropriately. Any configurations of type $b = \Delta a + \delta$ for arbitrary δ fulfills the algebraic relations, but to keep edge effects small δ must be smaller than any other coupling in the system. Choosing $\delta = \Delta$ is sufficient for this purpose. The preferred tight-binding models are such that the successive couplings are increased till a maximal coupling is reached, which is in contrast with the previous proposition.

The generation of mass.- Our scheme so far contemplates the appearance of a spectral gap corresponding to a finite mass in the DMO to result from an inherent asymmetry within the dimer, i.e. A and B have different eigenenergies. This produces the term $\mu\sigma_z$ in the hamiltonian [eq. (1)]. However, in practice an alternate option to generate a gap occurs due to finite size effects: We choose the smallest inter-dimer coupling to be slightly smaller, rather than equal to the intra-dimer coupling, i.e. $\Delta' \gtrsim \Delta_{\text{min}}$. Numerical inspection of the tight-binding model shows that, while a gap opens, the effects on the relative position of the eigenvalues on both sides of the gap have finite size errors similar to the ones in the gapless case. Note that the gap depends on the number of sites and vanishes as this number goes to infinity; therefore a large array will not describe a DMO with mass, in compliance with the chiral symmetry of the system [38]. Yet for finite sizes we do get the desired spectrum and we can make appropriate approximations or numerical calculations in the tight-binding model to explain this satisfactorily. Nevertheless we suggest to adapt the gap size to the experimental one rather than

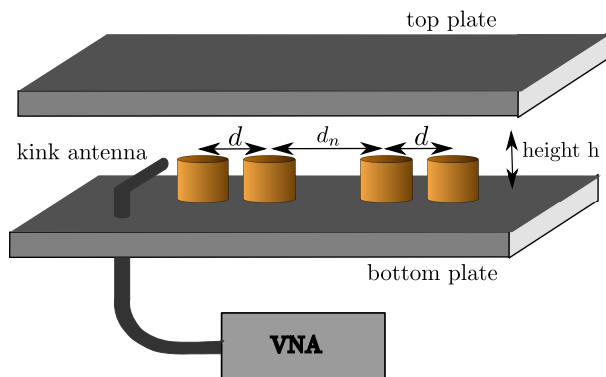


FIG. 2. Disks with a high index of refraction are placed between two metallic plates as a chain with center to center distances d_n or d . The microwaves are induced by a vector network analyzer (VNA) via a microwave cable and a kink antenna.

to get it from a tight-binding model as there will always remain discrepancies between the model and the experiment, which are entirely unrelated to the DMO. If we wish to take advantage of this finite size effect we should thus replace eq. (8) by

$$\epsilon_n = \pm \sqrt{\Delta^2 n + \mu_{\text{exp}}^2}, \quad (10)$$

where μ_{exp} refers to the parameter determined by the experiment.

Experimental results.— For the experimental realization of the DMO we use the techniques that have been developed to investigate the band structure of graphene [31–33]. The realization of the DMO is achieved as tight-binding system with nearest neighbor coupling and small higher order ones. A set of identical dielectric cylindrical disks (5 mm height, 4 mm radius and a refractive index of about 6) is placed between two metallic plates (see fig. 2). Close to one disk we placed a kink antenna connected to a vectorial network analyzer allowing to excite both transverse magnetic (TM) and transverse electric (TE) modes. The individual disks have an isolated TE resonance at 6.65 GHz. Restricting our investigation to frequencies around this value, where each disk contributes only one resonance. The electromagnetic field for this TE mode is mostly confined within the disks and spreads evanescently outside. A sketch of the experimental setup is shown in fig. 2 and a detailed description is presented in ref. [32].

In contrast to refs. [31, 32] we adjusted the height between the two plates to $h=13$ mm, to reduce the higher order neighbor couplings. The coupling parameter Δ between two adjacent disks depends on the distance between centers of the disks d and can be given in

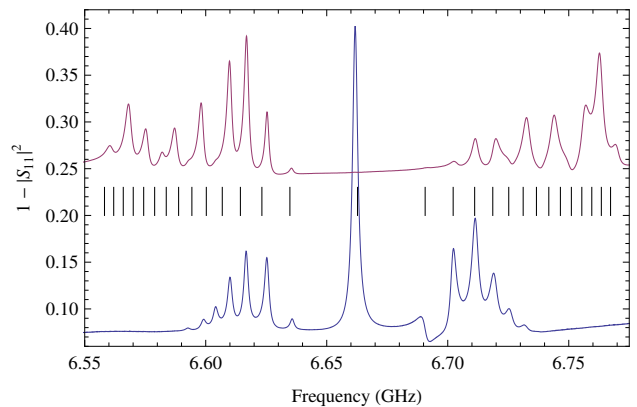


FIG. 3. Reflection spectra of a Dirac Oscillator without mass for a 15 dimer chain with minimal dimer distance of $d_{\text{min}} = 13$ mm. The upper spectrum (up-shifted) is measured at the 15th disk whereas the lower is measured at 3rd disk. The vertical lines indicate the predicted resonance positions from eq. (12) with $\Delta = 0.023$ GHz.

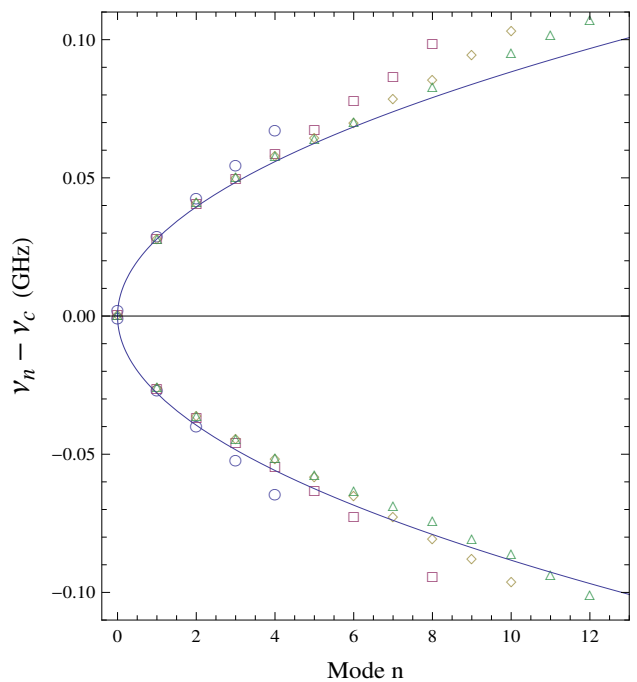


FIG. 4. Dirac-Moshinsky Oscillator without mass for an intra-dimer distance of 13 mm. The continuous curve correspond to the analytical prediction (12). The symbols correspond to different numbers of dimers: 6 dimers (circles), 9 dimers (squares), 12 dimers (diamonds), and 15 dimers (triangles).

terms of a modified Bessel function $|K_0|^2$, as described in [31, 32]. Thus, by changing the distance between disks, one changes the inter-disk couplings and obtains the 1D-DMO.

For the sake of simplicity let us assume an exponential law which is a good approximation of the coupling in terms of the distance in the range of interest. Then the

distances d_n between the dimers in the massless case are given by

$$d_n = -\frac{1}{\gamma} \ln \left(\frac{\Delta_n}{\Delta_K} \right) = -\frac{1}{\gamma} \ln \left(\frac{\Delta \sqrt{n}}{\Delta_K} \right). \quad (11)$$

The intra-dimer distance is d and we chose $d_1 = d$. The distances between the dimers are decreasing monotonically, thus the smallest possible distance d_{inf} determined by the diameter of the disks d_D defines the largest possible coupling Δ_{sup} and the largest allowable number of dimers n_{sup} giving the largest admissible size of our dimer chain. The number of energy levels is therefore equal to $2n_{\text{sup}}$. The eigenfrequencies for the 1D-DMO without mass is then given by

$$\nu_n = \nu_c \pm \Delta \sqrt{n}, \quad (12)$$

where ν_c is the eigenfrequency of a single disk. We used an intra-dimer distance d of 13, 14 and 15 mm and chains of 12, 18, 24 and 30 disks. In fig. 3 we show the reflection spectra for $d=13$ mm and 30 disks for two different antenna positions. The height of the resonances depends on the antenna site, as it is proportional to the intensity of the wavefunction at the disk. By measuring at different sites it is possible to extract all resonance positions. The vertical lines correspond to the theoretical predictions and a good agreement is found. Deviations increase at the edges of the spectrum, as designed by the choice of the cutoff.

We now investigate the dependence on the chain length. The measured eigenfrequencies as a function of the mode number is shown in fig. 4. The continuous curve corresponds to the analytical prediction (12). As the number of dimers increases, we find that the low levels are best reproduced by the theoretical curve (12) and the point of departure from theory moves further away from the center of the spectrum as the number of dimers increases. For dimer distances of 14 and 15 mm we got similar results. Thus we experimentally measured the spectrum of the Dirac-Moshinsky oscillator without mass in a finite approximation.

As we only have disks of the same type, meaning having approximately the same resonance frequency, we cannot directly generate the 1D-DMO with mass as originally introduced. But, as mentioned above, for a finite chain one can introduce a mass term by setting the intra-dimer coupling Δ' larger than the smallest coupling between the dimers Δ_{min} . Thus we only have to set the intra-dimer distance d to be smaller than the maximal inter-dimer distance d_1 . We used a chain of 15 dimers with an initial inter-dimer distance $d_1=15$ mm and a smallest inter-dimer distance $d_{14} = d_{\text{min}} \approx 10.81$. As intra-dimer distances d we choose 10, 11, and 12 mm. In fig. 5 we present the reflection spectra and the theoretical prediction (eq. (2)) for $d=10$ mm. We observe the expected gap at the center and find a good agreement

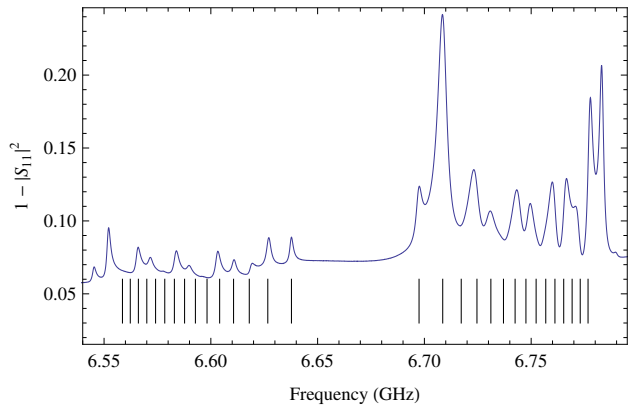


FIG. 5. Reflection spectrum of a Dirac-Moshinsky Oscillator with mass for a 15 dimer chain, where the intra-dimer distance of 10 mm and the inter-dimer distance of $d_{\text{min}} = 10.81$ mm. The vertical lines indicate the predicted resonance positions from eq. (12) with $\mu = 1.066$ GHz and $\Delta = 0.028$ GHz.

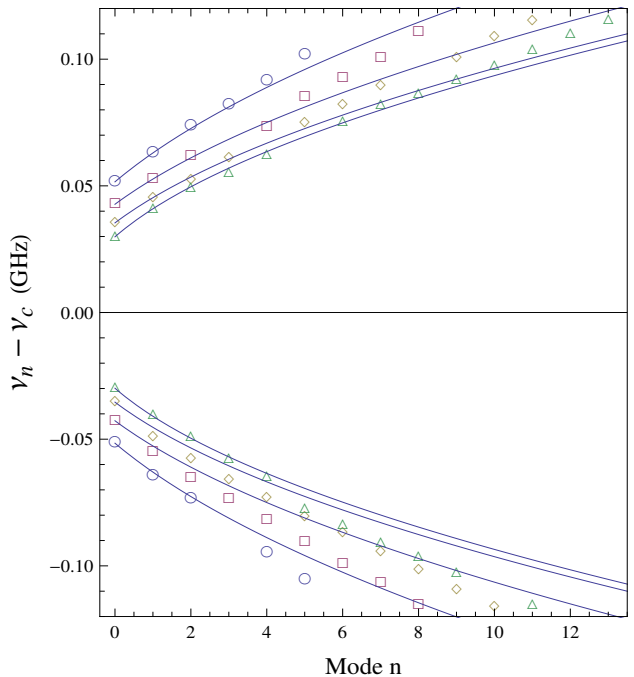


FIG. 6. Dirac oscillator with mass for different number of dimers, where the last dimers are removed. The intra-dimer distance is $d=10$ mm. Displayed are 6 ($d_{\text{min}} \approx 12.32$ mm, Circles), 9 ($d_{\text{min}} \approx 11.61$ mm, squares), 12 ($d_{\text{min}} \approx 11.15$ mm, diamonds), and 15 ($d_{\text{min}} \approx 10.81$ mm, triangles). Additionally the corresponding theoretical curves resulting from (9) are plotted as solid lines.

for the resonances close to the gap. Again the outer resonances show larger deviations. Next we removed step by step the last dimer, thus increasing the minimal inter-dimer distance d_{min} starting with d_{inf} .

In fig. 6 the resonances for different chain lengths are shown. We observe a good agreement for the upper spectrum with eq. (2). The two bands behave slightly differ-

ently, especially their width is different, due to the second nearest neighbor couplings, as was also observed in square and graphene lattices [39]. Furthermore the gap is observed to increase monotonically with d_{\min} .

In conclusion, we have experimentally realized the 1-D DMO based on the correspondence of the DMO to a tight-binding model. Within this model effects of finite size are small at the center of the spectrum. Furthermore, we have produced a gap in the spectrum which can be interpreted as the mass of the fermion. This was done by a distortion that applies only to finite arrays, as the infinite limit of the system makes such a gap vanish. We hope for the future to realize a 2D-DMO as mentioned in Ref. [30]. The model assumes a logarithmically deformed hexagonal lattice with only nearest neighbor couplings. To respect this coupling condition a realization of the 2-D DMO is not possible with our distance-coupling relation. However, microwave graphs seems to be a promising candidate [40, 41].

ACKNOWLEDGMENTS

T. H. S., J. A. F. V. and S. B. thank the University of Nice for the hospitality during several long term visits at the LPMC. T. H. S. and J. A. F. V. to CONACyT Project Number 79613, PAPIIT-UNAM project number IG101113 and PAEP-UNAM for financial supports. E. S. acknowledges support from PROMEP project No. 103.5/12/4367.

-
- [1] D. Itô, K. Mori, and E. Carriere, *Nuovo Cimento*, **51 A**, 1119 (1967).
- [2] P. A. Cook, *Nuovo Cimento*, **1**, 149 (1971).
- [3] M. Moshinsky and A. Szczepaniak, *J. Phys. A*, **22**, L817 (1989).
- [4] E. Sadurní, *AIP Conf. Proc.*, **1334**, 249 (2010).
- [5] J. M. Torres, E. Sadurní, and T. H. Seligman, *AIP Conf. Proc.*, **1323**, 301 (2010).
- [6] M. Hamzavi, M. Eshghi, and S. M. Ikhdair, *J. Math. Phys.*, **53**, 082101 (2012).
- [7] C.-K. Lu and I. F. Herbut, *J. Phys. A*, **44**, 295003 (2011).
- [8] S. Zarrinkamar, A. A. Rajabi, and H. Hassanabadi, *Annals of Physics*, **325**, 2522 (2010).
- [9] Y. Chargui, A. Trabelsi, and L. Chetouani, *Phys. Lett. A*, **374**, 2907 (2010).
- [10] A. Bermudez, M. A. Martin-Delgado, and A. Luis, *Phys. Rev. A*, **77**, 063815 (2008).
- [11] D. A. Kulikov, R. S. Tutik, and A. P. Yaroshenko, *Phys. Lett. B*, **644**, 311 (2007).
- [12] A. S. de Castro, P. Alberto, R. Lisboa, and M. Malheiro, *Phys. Rev. C*, **73**, 054309 (2006).
- [13] A. C. Alhaidari, H. Bahlouli, and A. Al-Hasan, *Phys. Lett. A*, **349**, 87 (2006).
- [14] C. Quesne and V. M. Tkachuk, *J. Phys. A*, **38**, 1747 (2005).
- [15] C. L. Ho and P. Roy, *Annals of Physics*, **312**, 161 (2004).
- [16] R. Lisboa, M. Malheiro, A. S. de Castro, and et al., *Phys. Rev. C*, **69**, 024319 (2004).
- [17] A. D. Alhaidari, *J. Phys. A*, **34**, 9827 (2001).
- [18] A. D. Alhaidari, *Phys. Rev. Lett.*, **87**, 210405 (2001).
- [19] J. Benitez, R. P. Martinez y Romero, H. N. Nunezyppez, and et al., *Phys. Rev. Lett.*, **64**, 1643 (1990).
- [20] J. Munarriz, F. Dominguez-Adame, and R. P. A. Lima, *Phys. Lett. A*, **376**, 3475 (2012).
- [21] J. Grineviciute and D. Halderson, *Phys. Rev. C*, **85**, 054617 (2012).
- [22] A. Faessler, V. I. Kukulkin, and M. A. Shikhalev, *Annals of Physics*, **320**, 71 (2005).
- [23] Y. X. Wang, J. Cao, and S. J. Xiong, *Eur. Phys. J. B*, **85**, 237 (2012).
- [24] E. Romera, *Phys. Rev. A*, **84**, 052102 (2011).
- [25] V. V. Dodonov, *J. Opt. B*, **4**, R1 (2002).
- [26] A. Bermudez, M. A. Martin-Delgado, and E. Solano, *Phys. Rev. Lett.*, **99**, 123602 (2007).
- [27] L. Lamata, J. León, T. Schätz, and E. Solano, *Phys. Rev. Lett.*, **98**, 253005 (2007).
- [28] S. Longhi, *Opt. Lett.*, **35**, 1302 (2010).
- [29] F.-L. Zhang, B. Fu, and J.-L. Chen, *Phys. Rev. A*, **80**, 054102 (2009).
- [30] E. Sadurní, T. Seligman, and F. Mortessagne, *New J. of Physics*, **12**, 053014 (2010).
- [31] U. Kuhl, S. Barkhofen, T. Tudorovskiy, H.-J. Stöckmann, T. Hossain, L. de Forges de Parny, and F. Mortessagne, *Phys. Rev. B*, **82**, 094308 (2010).
- [32] S. Barkhofen, M. Bellec, U. Kuhl, and F. Mortessagne, *Phys. Rev. B*, **87**, 035101 (2013).
- [33] M. Bellec, U. Kuhl, G. Montambaux, and F. Mortessagne, *Phys. Rev. Lett.*, **110**, 033902 (2013).
- [34] M. Moshinsky, G. Loyola, A. Szczepaniak, C. Villegas, and N. Aquino, "The Dirac oscillator and its contribution to the baryon mass formula," in *Rio de Janeiro 1989, Relativistic aspects of nuclear physics* (World Scientific Press, Singapore, 1990) p. 271.
- [35] M. Moshinsky, G. Loyola, and C. Villegas, in *Group Theoretical Methods in Physics*, Lecture Notes in Physics, Vol. 382, edited by V. Dodonov and V. Man'ko (Springer Berlin Heidelberg, 1991) p. 339.
- [36] M. Moshinsky, G. Loyola, and A. Szczepaniak, "The two body Dirac oscillator," in *J J Giambiagi Festschrift*, edited by H. Falomir (World Scientific Publishing Co Pte Ltd, 1991).
- [37] M. Moshinsky and Y. Smirnov, *The Harmonic Oscillator in Modern Physics*, Proc. of the Rio de Janeiro Int. Workshop on Relativistic Aspects of Nucl. Phys. (Hardwood Academic Publishers, Amsterdam, 1996).
- [38] G. Semenoff, *Phys. Scr.*, **T146**, 014016 (2012).
- [39] M. Bellec, U. Kuhl, G. Montambaux, and F. Mortessagne, "Band structure deformations due to high-order coupling in photonic artificial graphene," To be published.
- [40] O. Hul, S. Bauch, P. Pakoński, N. Savvitsky, K. Życzkowski, and L. Sirko, *Phys. Rev. E*, **69**, 056205 (2004).
- [41] O. Hul, O. Tymoshchuk, S. Bauch, P. Koch, and L. Sirko, *J. Phys. A*, **38**, 10489 (2005).